Institutionen för systemteknik
Department of Electrical Engineering

Examensarbete

Motion Tracking Using a Permanent Magnet

Examensarbete utfört i Biomedical Engineering
vid Tekniska högskolan vid Linköpings universitet
av

Jacob Antonsson

LiTH-ISY-EX--13/4697--SE

Linköping 2013

Linköpings universitet
TEKNISKA HÖGSKOLAN

Department of Electrical Engineering
Linköpings universitet
SE-581 83 Linköping, Sweden

Linköpings tekniska högskola
Linköpings universitet
581 83 Linköping

Motion Tracking Using a Permanent Magnet

Examensarbete utfört i Biomedical Engineering
vid Tekniska högskolan vid Linköpings universitet
av

Jacob Antonsson

LiTH-ISY-EX--13/4697--SE

Handledare: **Henk Kortier**
BIOMEDICAL SIGNALS AND SYSTEMS, Universiteit Twente
Niklas Wahlström
ISY, Linköpings universitet

Examinator: **Fredrik Gustafsson**
ISY, Linköpings universitet
Peter Veltink
BIOMEDICAL SIGNALS AND SYSTEMS, Universiteit Twente

Linköping, 7 juni 2013

Avdelning, Institution
Division, Department

Automatic Control
Department of Electrical Engineering
SE-581 83 Linköping

Datum
Date

2013-06-07

Språk
Language

☐ Svenska/Swedish
☒ Engelska/English

☐ ________________

Rapporttyp
Report category

☐ Licentiatavhandling
☒ Examensarbete
☐ C-uppsats
☐ D-uppsats
☐ Övrig rapport
☐ ________________

ISBN
—

ISRN
LiTH-ISY-EX--13/4697--SE

Serietitel och serienummer
Title of series, numbering

ISSN
—

URL för elektronisk version

`http://urn.kb.se/resolve?urn=urn:nbn:se:liu:diva-94591`

Titel
Title

Svensk titel

Motion Tracking Using a Permanent Magnet

Författare
Author

Jacob Antonsson

Sammanfattning
Abstract

In this project the possibility of using a network of magnetometers sensing a permanent magnet for tracking has been investigated. Both the orientation and the position of the magnet have been considered. A dipole approximation of the magnetic field is used to develop two models. One of the models parametrizes the orientation with the magnetic moment vector, while the other parametrizes the orientation with a unit quaternion. An extended Kalman filter have been used to estimate position and orientation.

Several calibration algorithms have been developed to calibrate for sensor errors, differences in sensor coordinate frame orientations and also for the estimation of the magnetic moment norm of a permanent magnet. The models have been tested using an optical reference system for position and orientation estimation. Initial results are ambiguous and further testing is necessary. One conclusion is that the model using the magnetic moment vector as orientation parametrization is less sensitive to the accuracy of the initial guesses of the filter recursions and also less sensitive to possible model errors.

A mathematical result of the possibility of using a non stationary sensor network to track the magnet is also given.

Nyckelord
Keywords

problem, lösning

Abstract

In this project the possibility of using a network of magnetometers sensing a permanent magnet for tracking has been investigated. Both the orientation and the position of the magnet have been considered. A dipole approximation of the magnetic field is used to develop two models. One of the models parametrizes the orientation with the magnetic moment vector, while the other parametrizes the orientation with a unit quaternion. An extended Kalman filter have been used to estimate position and orientation.

Several calibration algorithms have been developed to calibrate for sensor errors, differences in sensor coordinate frame orientations and also for the estimation of the magnetic moment norm of a permanent magnet. The models have been tested using an optical reference system for position and orientation estimation. Initial results are ambiguous and further testing is necessary. One conclusion is that the model using the magnetic moment vector as orientation parametrization is less sensitive to the accuracy of the initial guesses of the filter recursions and also less sensitive to possible model errors.

A mathematical result of the possibility of using a non stationary sensor network to track the magnet is also given.

Sammanfattning

Ett sensornätverk med magnetometrar har använts för estimering av position och orientering av en permanent magnet. En dipolapproximation av det magnetiska fältet från magneten har använts för att härleda två modeller för detta ändamål. En av modellerna parametriserar orienteringen med magnetens magnetiska momentvektor. Den andra använder en enhetskvaternion för att representera magnetens orientering.

Kalibreringsrutiner har utvecklats som kalibrerar för sensorfel, skillnader i orientering hos sensorerna och även för estimering av normen hos magnetens magnetiska momentvektor. Ett optiskt referenssystem för estimering av position och orientering har använts för att validera modellerna. Resultaten är inte entydiga och det är tydligt att fler tester behöver göras. En slutsats är att modellen som parametriserar orienteringen med den magnetiska momentvektorn är mindre känslig för fel i mätdata och startgissningar för filtret. Ett matematiskt resultat om möjligheten att använda ett rörligt sensornätverk för att estimera position och orientering hos magneten ges också.

Contents

1 Introduction **5**
1.1 Project Description . . . 6
1.2 Related Work . . . 7
1.3 Comments . . . 8

2 Theoretical Preliminaries **9**
2.1 Motion Models for Tracking . . . 10
2.2 Linear Estimation . . . 11
2.3 The Extended Kalman Filter . . . 11
2.4 A Brief Note on 3D Orientation . . . 13

3 Modelling **15**
3.1 The Relaxed Model . . . 16
3.2 The Constrained Model . . . 18
3.3 Toward a Non Stationary Sensor Network . . . 21

4 Calibration **25**
4.1 Gain and Sensor Reading Errors . . . 25
4.2 Frame Differences . . . 26
4.3 Position Calibration . . . 27
4.4 Magnetic Moment Norm . . . 28
4.5 Sensor Covariance Estimation . . . 29

5 Validation **31**
5.1 Acquiring Ground Truth Measurements . . . 32
5.2 Tracking Comparison for the Relaxed Model . . . 34
5.3 Proof of Concept for the Constrained Model . . . 34
5.4 Discussion . . . 35

6 Conclusions **43**
6.1 Further work . . . 44

Bibliography **45**

1

Introduction

Systems for tracking human movement are used for several purposes such as entertainment, systems like Microsoft Kinect and the Wii gaming console are examples of this, surveillance and virtual reality. Human motion tracking is also of interest in many scientific disciplines such as sports science and biomechanics. Human motion is also of particular interest for the field of medicine and biomedical engineering. There are a lot of pathologies where the moving pattern of patients are of interest; knowing such patterns alleviates diagnosis, makes it possible to monitor the condition of a patient to see if it is deteriorating and also to gain insight in how the pathology affects the dexterity and balance of the subject. Real-time knowledge of the movement of a patient can also be used for example to design routines for efficient rehabilitation.

Human motion tracking has traditionally been done using optical measurement systems. Such systems tend to be expensive and complex, and they require line-of-sight to the target. Optical systems such as Vicon or Optotrak are considered to be the golden reference standard of human motion tracking.

More recently magnetic and inertial sensing have been used to track ambulatory motion in a statistical signal processing framework [Schepers, 2009, Roetenberg, 2006]. Inertial sensing has traditionally been used by the navigation community for orientation and position estimation for aircraft and ships. The sensors for such applications are often expensive and unwieldy. With the development of micro-machined electromechanical system (MEMS) technology however, inertial and magnetic sensors have become so small and cheap that they are now used in plenty of products intended for the consumer market such as smart phones and video game consoles. This development for inertial sensors has made the use of inertial and magnetic sensing viable for ambulatory applications.

An inertial measurement unit (IMU) consists of a three dimensional (3D) accelerometer, a 3D gyro and sometimes also a 3D magnetometer. For strap-down navigation the IMU are strapped to a body. The gyro and the accelerometer of the IMU can then be used to get the angular velocity and the linear acceleration of the body. Ostensibly the orientation and the position can then be acquired by integrating the angular velocity and double-integrating the linear acceleration respectively. When an estimate is integrated the estimation error is integrated with it however, giving increasingly larger errors leading to so called integration drift. This is especially a problem for the estimation of position using acceleration measurements since the acceleration signal needs to be integrated twice.

The inertial measurement units used for this work are the Xsens MTw's shown in Figure 1.1. Primarily the magnetometers in the sensors have been used. The gyro and the accelerometer have only been used for the position calibration detailed in Section 4.3

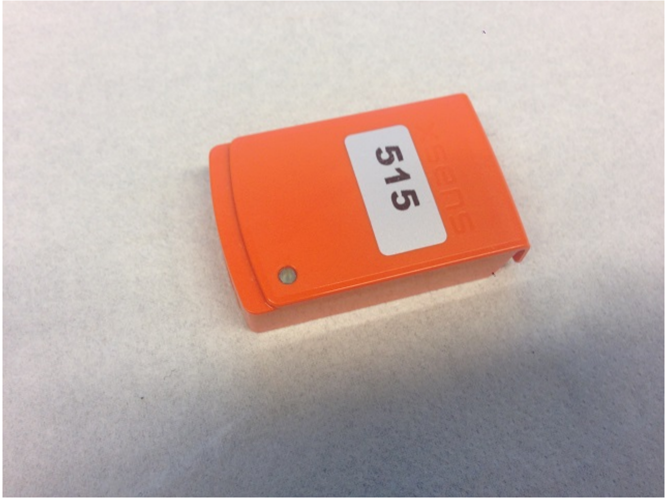

Figure 1.1: *Xsens MTw sensor*

1.1 Project Description

In this work a novel approach is used to get reliable position and orientation (pose) estimates from a moving target. This is done by measuring the magnetic field from a permanent magnet with a sensor network of magnetometers. By describing the magnetic field of the magnet as a magnetic dipole field it is possible to relate the relative position and orientation of the magnet with respect to the magnetometer network to the magnetometer measurements. The relative position and the orientation of the magnet can then be reconstructed solving the inverse problem for example using a statistical filter.

Two different models of varying complexity are constructed for pose estimation using a permanent magnet with a sensor network of magnetometers. The models are validated using an optical reference system. Some calibration routines are also developed to shape the measurements so that they fit as closely to the models as possible.

The models are firstly constructed for the setting where the sensor network is stationary and the coordinate frame of the sensor network is oriented according to the world coordinate system. Some mathematical results are then proved regarding the possibility of using the same models for a sensor network with a frame oriented differently than the world frame, and possibly also moving. The moving tracking system is not tested in practice due to time constraints, and practical constraints of the optical validation system.

The developed models are intended to be used in the application of human motion tracking. By fastening the magnet to the hand it is possible to use the models to track the movement of the hand in a tracking volume around the stationary sensor network. By strapping the sensor network to the chest it should be possible to track the movement of the hand in an ambulatory setting.

1.2 Related Work

A vast literature exist in the field of human motion analysis see [Zhou and Hu, 2008] for a survey. For an example of a typical modern approach to orientation estimation of human limbs using both inertial and magnetic measurements with an extended Kalman filter see [Yun and Bachmann, 2006] and [Roetenberg et al., 2005]. In [Roetenberg et al., 2007a] a portable position and orientation tracker is developed. An electric coil is used for the magnetic signal, requiring extra hardware and access to energy, limiting the time the system can be used however and to make sense of the magnetic field of the earth in the moving sensor frame orientation measurements from an IMU are used. In [Roetenberg et al., 2007b] a sensor network of IMUs is used with the magnetic coil system as an aid to minimize the energy requirements of the system and still get accurate position and orientation estimation. The tracking system in [Roetenberg et al., 2007a,b] models the actuated magnetic source as a dipole, but it does not incorporate a description of the measurement noise and does not utilize an optimal filtering framework. It also involves three actuated orthogonally mounted source coils adding to the complexity of system.

Building on this work in [Schepers and Veltink, 2010, Schepers et al., 2010] some of these issues are addressed. In [Schepers and Veltink, 2010] a stochastic magnetic measurement model is developed for use in an optimal filtering framework with just one active magnetic source coil. In [Schepers et al., 2010] a system that fuses inertial and magnetic measurements using optimal filtering is developed with the model from [Schepers and Veltink, 2010]. Moreover it addresses the energy problem by minimizing the amount of magnetic actuations needed using an adaptive actuation framework.

The idea of using a dipole model for the magnetic field of a permanent magnet for localization and tracking appears in [Birsan, 2003], where the application is to detect and track ships in shallow waters and near shores where traditional acoustic methods for this purpose is not as applicable. Several nonlinear filters are evaluated for the tracking of a permanent magnet but only on data simulated from a dipole model with added noise. In [Callmer et al., 2010] a dipole model is used for sensor localization under water. A dipole model of a ferromagnetic object is also used in [Wahlström, 2013] for the detection and tracking of metallic targets, particularly cars. Included there is also a discussion of the validity of the model for a static sensor network; one conclusion is that at least two sensors are needed for full observability of both position and orientation of the permanent magnet.

1.3 Comments

The orientation estimation of the filters developed in this project is not tested with ground truth measurements due to time limitations. Such ground truth measurements are available however and such a comparison could be made in the future. Also note that the position calibration algorithm of the sensors outlined in Section 4.3 is wholly the work of one of my supervisors Henk Kortier. Both the idea and the implementation are his. A future publication of the algorithm is planned.

2

Theoretical Preliminaries

Target tracking is usually done using a statistical filter. A statistical filter is a recursive algorithm that uses information about the physical behaviour of a system and the measurements of the system to reconstruct its underlying physical quantities. The information of the behaviour of the system can often be described mathematically as a state space model. A state space model is an abstract description of a system consisting of two equations relating the input, the noise, and the output of the system with its underlying physical variables, traditionally called states. One equation describes the dynamics of the system, how the states change in time, by a first order differential equation where the derivative of the state vector is related to the state vector, the input and the system noise; this relation is called the dynamical equation, or the system equation. The other equation relates the output to the states and possible measurement noise; this equation is called the measurement equation. Considering only cases where the two equations have explicit expressions a continuous state space model is written

$$\dot{x}(t) = f(x(t), w(t), u(t), \theta, t) \tag{2.1a}$$

$$y(t) = h(x(t), e(t), u(t), \theta, t) \tag{2.1b}$$

where $x(t)$ is a vector of the state variables, $w(t)$ and $e(t)$ are independent stochastic variables describing the system noise and the measurement noise respectively, $u(t)$ is a known input, θ is a vector of parameters and t as usual denotes time.

In filtering applications physical quantities of the system are measured by sensors. In this setting the measurement equation (2.1b) describes how the actual physical measurements are related to the states of the system. The filter then uses this relation to reconstruct the states by predicting the measurements and then comparing these predictions with the actual measurements. In a practical situation the sensors usually collect samples of some quantities of the system, i.e.

they work in discrete time. The dynamical equation is often given in continuous time and thus needs to be discretized to discrete time for use in a computer-implemented filter. In most applications the filtering problem can be greatly simplified by assuming that the system and measurement noise is additive and Gaussian. Also for the purposes of tracking the inputs to the system is usually unknown and modelled as Gaussian stochastic processes and the time dependency of the system and measurement equations can be dropped. Considering all this the typical state space model for a tracking-problem is on the form

$$x_{k+1} = f(x_k) + G_k w_k, \qquad w_k \in N(0, Q) \tag{2.2a}$$

$$y_k = h(x_k) + e_k, \qquad e_k \in N(0, R) \tag{2.2b}$$

where $f(\ )$ and $h(\ )$ are nonlinear functions and G_k is a possibly time-varying matrix.

2.1 Motion Models for Tracking

The typical states for a tracking system are position, linear velocity, linear acceleration, orientation and angular velocity. In this work only position, linear velocity, orientation and angular velocity are used. Denote position by $p(t)$ and linear velocity by $v(t)$. Nothing is known about the velocity of the system so the dynamics of the velocity is modelled as random walk. This give the following dynamic model

$$\begin{pmatrix} \dot{p} \\ \dot{v} \end{pmatrix} = \underbrace{\begin{pmatrix} 0 & I \\ 0 & 0 \end{pmatrix}}_{A} \begin{pmatrix} p \\ v \end{pmatrix} + \underbrace{\begin{pmatrix} 0 \\ 1 \end{pmatrix}}_{B} w^v(t), \quad w^v(t) \in N(0, Q^v) \tag{2.3}$$

Note that $A^n = 0, n \geq 2$. It is well known, see for example [Gustafsson, 2010, Törnqvist, 2008], that the discrete time counterpart of this continuous dynamical system, assuming zero order hold (ZOH) sampling i.e. that the noise-input is constant over a sampling interval $t = kT < \tau < t + T = (k+1)T$, is given by

$$\begin{pmatrix} p_{k+1} \\ v_{k+1} \end{pmatrix} = F \begin{pmatrix} p_k \\ v_k \end{pmatrix} + G w_k, \quad w_k^v \in N(0, Q^v) \tag{2.4}$$

where

$$F = \exp(AT) = I + AT + \frac{(AT)^2}{2!} + \frac{(AT)^3}{3!} + \cdots = I + AT =$$
$$= \begin{pmatrix} I & TI \\ 0 & I \end{pmatrix}$$

and

$$G = \int_0^T \exp(A\tau)B\,d\tau = \left(IT + \frac{AT^2}{2!} + \frac{A^2T^3}{3!} + \cdots\right)B =$$
$$= \left(IT + \frac{AT^2}{2!}\right)B = \begin{pmatrix} IT & IT^2/2 \\ 0 & IT \end{pmatrix}\begin{pmatrix} 0 \\ 1 \end{pmatrix} = \begin{pmatrix} IT^2/2 \\ IT \end{pmatrix}$$

This kind of motion model is called a constant velocity model. Let m be a state with dynamics modelled as random walk, i.e.

$$\dot{m} = w^m(t), \quad w^m(t) \in N(0, Q^m) \tag{2.5}$$

Analogously to the above calculations the discrete time model using ZOH is given by

$$m_{k+1} = m_k + Tw_k^m, \quad w_k^m \in N(0, Q^m) \tag{2.6}$$

2.2 Linear Estimation

The filtering problem is to find the best estimate of the state x_k at the time k based on all measurements up to and including the time-instant k, $y_{1:k}$. Denote the estimate of the state at time k given measurements up until the time instant m by $\hat{x}_{k|m}$. Similarly denote the covariance of this estimate $P_{k|m}$. There exist only a few analytical solutions for the filtering problem. The most important analytical solution is the linear filter that gives the estimate $\hat{x}_{k|k}$ with the minimum variance for a linear time-discrete Gaussian system with Gaussian prior

$$\begin{aligned} x_{k+1} &= F_k x_k + G_{u,k} u_k + G_{w,k} w_k, \quad w_k \in N(0, Q_k) \\ y_k &= H_k x_k + D_k u_k + e_k, \quad e_k \in N(0, R_k) \\ x_0 &\in N(\hat{x}_{1|0}, P_{1|0}) \end{aligned}$$

where, w_k and e_k are uncorrelated and u_k is the system input as usual. The solution to the linear filtering problem for this system is the well-known Kalman filter given in Algorithm 1. For more information see for example [Gustafsson, 2010, Kailath et al., 2000] The minimum-variance linear filter has an analytical solution for a linear Gaussian state space model because a linear combination of Gaussian variables is also a Gaussian variable, see [Gut, 2009] for further information.

2.3 The Extended Kalman Filter

For the nonlinear model 2.2 there is no analytical solution to the optimal filtering problem. A common solution is to linearize the model using a first order Taylor expansion and then use the Kalman filter. Given an estimate $\hat{x}$ of the state the

Algorithm 1 The Kalman Filter

Initialize

$$\hat{x}_{1|0} = \mathrm{E}(x_0)$$
$$P_{1|0} = \mathrm{Cov}(x_0)$$

Measurement update

$$S_k = H_k P_{k|k-1} H_k^T + R_k \tag{2.7a}$$
$$K_k = P_{k|k-1} H_k^T S_k^{-1} \tag{2.7b}$$
$$\varepsilon_k = y_k - H_k \hat{x}_{k|k-1} - D_k u_k \tag{2.7c}$$
$$\hat{x}_{k|k} = x_{k|k-1} + K_k \varepsilon_k \tag{2.7d}$$

Time update

$$\hat{x}_{k+1|k} = F_k \hat{x}_{k|k} + G_{u,k} u_k \tag{2.7e}$$
$$P_{k+1|k} = F_k P_{k|k} F_k^T + G_{v,k} Q_k G_{v,k}^T \tag{2.7f}$$

first order Taylor expansion of the model is given by

$$\begin{aligned} x_{k+1} &\approx f(\hat{x}_k) + f'(\hat{x}_k)(x_k - \hat{x}_k) + G_k w_k = \qquad &(2.8a)\\ &= f'(\hat{x}_k)x_k + f(\hat{x}_k) - f'(\hat{x}_k)\hat{x}_k + G_k w_k &(2.8b)\\ y_k &\approx h(\hat{x}_k) + h'(\hat{x}_k)(x_k - \hat{x}_k) + e_k = h'(\hat{x}_k)x_k + h(\hat{x}_k) - h'(\hat{x}_k)\hat{x}_k + e_k &(2.8c) \end{aligned}$$

where h' and f' denotes the Jacobians of the functions f and h respectively and $w_k \in N(0, Q)$ and $e_k \in N(0, R)$ are uncorrelated. The extended Kalman filter is obtained by linearizing in the recursion around the current estimate, $\hat{x}_{k|k}$ for the time-update and $\hat{x}_{k|k-1}$ for the measurement update. The constant terms $f(\hat{x}_{k|k}) - f'(\hat{x}_{k|k})\hat{x}_{k|k}$ and $h(\hat{x}_{k|k-1}) - h'(\hat{x}_{k|k-1})\hat{x}_{k|k-1}$ can be seen as inputs to the system. The resulting recursions are given in Algorithm 2.

Algorithm 2 The Extended-Kalman Filter

Initialize

$$\hat{x}_{1|0} = \mathrm{E}(x_0)$$
$$P_{1|0} = \mathrm{Cov}(x_0)$$

Measurement update

$$S_k = h'(\hat{x}_{k|k}) P_{k|k-1} h'(\hat{x}_{k|k})^T + R_k \tag{2.9a}$$
$$K_k = P_{k|k-1} h'(\hat{x}_{k|k})^T S_k^{-1} \tag{2.9b}$$
$$\begin{aligned} \varepsilon_k &= y_k - h'(\hat{x}_{k|k})\hat{x}_{k|k-1} - (h(\hat{x}_{k|k-1}) - h'(\hat{x}_{k|k-1})\hat{x}_{k|k-1}) = \qquad &(2.9c)\\ &= y_k - h(\hat{x}_{k|k-1}) &(2.9d) \end{aligned}$$
$$\hat{x}_{k|k} = x_{k|k-1} + K_k \varepsilon_k \tag{2.9e}$$

Time update

$$\hat{x}_{k+1|k} = f'(\hat{x}_{k|k})\hat{x}_{k|k} + f(\hat{x}_{k|k}) - f'(\hat{x}_{k|k})\hat{x}_{k|k} = f(\hat{x}_{k|k}) \tag{2.9f}$$
$$P_{k+1|k} = f'(\hat{x}_{k|k}) P_{k|k} f'(\hat{x}_{k|k})^T + G_k Q_k G_k^T \tag{2.9g}$$

The first order Taylor expansions in 2.8 neglect a second order rest-term. This approximation works well as long as either the model is almost linear, so that the Hessians of the functions f and h are close to zero, or if the model is very accurate, the initial guesses are good and the signal-to-noise ratio is high. The extended Kalman filter is more or less an ad-hoc solution. Very few results about convergence or theoretical bounds on the performance of the filter exists. For more details on this see for example [Gustafsson, 2010, Kailath et al., 2000].

2.4 A Brief Note on 3D Orientation

In tracking problems it is often needed to find a parametrization that describes the relation between a vector given in two different coordinate systems. Denote the vector v given in the coordinate frame Ψ_a by v^a. Let Ψ_b be another frame with the same origin as Ψ_a. Let R^{ab} be a transformation such that

$$v^a = R^{ab} v^b \tag{2.10}$$

The transformation R^{ab} represents the orientation of the frame Ψ_b with respect to the frame Ψ_a. The question is how to best parametrize this transformation. If the orientation of the b-frame with respect to the a-frame is changing in time the complexity of the kinematics of the parametrization also needs to be considered. A first attempt to represent the orientation could be to use a rotation matrix, i.e. a matrix in the special orthogonal group $R^{ab} \in SO_3$, where

$$SO_3 \in \{R \in \mathbb{R}^{3\times 3} : RR^T = I \wedge \det(R) = 1\}$$

To parametrize a rotation matrix at least six parameters are needed. This fact along with the need to ensure the orthogonality constraints makes this parametrization practically infeasible. A more convenient parametrization is given by the fact that any rotation matrix can be factorized to three matrices where each matrix represents how one of the principal axes of the b-frame is rotated with respect to the principal axis of the a-frame. Such a matrix is a function of the rotation angles; the so called Euler angles. For example a rotation taken first an angle ψ around the z-axis, then an angle θ around the y-axis and lastly an angle ϕ around the x-axis gives the so called aerospace sequence

$$R^{ab} = R(x^b, \phi) R(y^b, \theta) R(z^b, \psi)$$

For complete derivations and explicit expressions of the matrices see [Kuipers, 2002]. This parametrization uses three parameters and the kinematic equations are relatively simple. The kinematic equations do have singularities at $\theta = \pm\frac{\pi}{2}$, see [Gustafsson, 2010], however making also this parametrization impractical.

The standard parametrization is to use the so-called quaternions. A quaternion can be represented by a four component vector $q = \begin{pmatrix} q_0 & q_1 & q_2 & q_3 \end{pmatrix}^T$. The key idea is that a rotation of a vector v^b can be written as the 'sandwich'-product between the quaternion representation of the vector $\bar{v} = \begin{pmatrix} 0 & v \end{pmatrix}^T$ and a unit quaternion

$$q^{ab} \bar{v} (q^{ab})^* \tag{2.11}$$

where q^* is the conjugate quaternion of q and $q^T q = 1$. For more information and the proper definition of the quaternion and operations on quaternions see [Kuipers, 2002] as a standard reference. By using the definition for quaternion multiplication (2.11) can be written as an orientation matrix in the quaternion q^{ab}, let for simplicity $q^{ab} = q$,

$$R^{ab}(q) = \begin{pmatrix} q_0^2 + q_1^2 - q_2^2 - q_3^2 & 2q_1q_2 + 2q_0q_3 & 2q_1q_3 - 2q_0q_2 \\ 2q_1q_2 - 2q_0q_3 & q_0^2 - q_1^2 + q_2^2 - q_3^2 & 2q_2q_3 + 2q_0q_1 \\ 2q_1q_3 + 2q_0q_2 & 2q_2q_3 - 2q_0q_1 & q_0^2 - q_1^2 - q_2^2 + q_3^2 \end{pmatrix} \tag{2.12}$$

Let $\omega_{ab}^b = \begin{pmatrix} \omega_x & \omega_y & \omega_z \end{pmatrix}$ be the angular velocity of orientation between the b-frame and the a-frame given in the b-frame. The dynamics of the quaternion is then given by

$$\dot{q}_{ab} = \frac{1}{2} \underbrace{\begin{pmatrix} 0 & -\omega_x & -\omega_y & -\omega_z \\ \omega_x & 0 & \omega_z & -\omega_y \\ \omega_y & -\omega_z & 0 & \omega_x \\ \omega_z & \omega_y & -\omega_x & 0 \end{pmatrix}}_{S(\omega_{ab}^b)} \begin{pmatrix} q_0 \\ q_2 \\ q_2 \\ q_3 \end{pmatrix} = \tag{2.13a}$$

$$= \frac{1}{2} \underbrace{\begin{pmatrix} -q_1 & -q_2 & -q_3 \\ q_0 & -q_3 & q_2 \\ -q_2 & q_1 & q_0 \end{pmatrix}}_{\bar{S}(q^{ab})} \begin{pmatrix} \omega_x \\ \omega_y \\ \omega_z \end{pmatrix} \tag{2.13b}$$

A closed form discretized version of this differential equation can be found using ZOH sampling, see for example [Törnqvist, 2008].

3

Modelling

To get an estimation of the pose of the magnet a state space model modelling both the dynamics of the magnet and the measurements of the magnetic field done by the magnetometers is needed. The magnetic field of the magnet can be approximated with a dipole field if the distance from the magnet to the magnetometers is far enough [Wahlström, 2013]. In Definition 3.1 a needed help function is defined

3.1 Definition.

$$J(r) \triangleq \frac{1}{\|r\|^5}\left(3rr^T - \|r\|^2 I\right)$$

Let $\tilde{r}^i$ be the relative position of the magnet and the ith magnetometer and m the magnetic moment of the magnet at one instance. The dipole field measured from the ith magnetometer at that instance is then given by

$$J(\tilde{r}^i)m \tag{3.1}$$

The actual magnetic field sensed by the magnetometer is a superposition of this field and a static field consisting of the magnetic field of earth possibly disturbed by magnetic materials in the vicinity of the magnetometer. If measurements are done indoors such disturbances will always be present. Denote this static field by B. The measurement y_k^i from the ith sensor at time k is given by (3.1) along with the additive bias term

$$y_k^i = B + J(\tilde{r}_k^i)m_k \tag{3.2}$$

The magnetic moment vector m of the magnet is only dependent on the orientation of the magnet. The orientation can thus be parametrized by the moment vector. The dipole field is invariant to rotation around the axis of this moment vector, so only 2 degrees of freedom DoF are observable. In [Wahlström, 2013] it is showed that to have full observability of position, linear velocity and the two DoF of the orientation of the magnet at least two magnetometers are needed. Magnetometers have a threshold for how strong a magnetic field they can measure before they are saturated. Therefore to ensure full observability and to make sure that the system can handle tracking of the magnet even when the magnet is close to the sensor network four magnetometers are used. In this way the filter can just discard measurements from a magnetometer if the magnet is too close to it and still have observability.

3.1 The Relaxed Model

A sketch of the situation to be modelled is shown in Figure 3.1. Nothing is known about the velocity of the magnet so a constant velocity model as outlined in Section 2.1 is used for the position and linear velocity of the magnet. In this model orientation is parametrized with the moment vector. The dynamics of the moment vector is modelled as random walk. Introduce the state vector

$$x_k = \begin{pmatrix} r_k^T & v_k^T & m_k^T & B_k^T \end{pmatrix}^T \tag{3.3}$$

where r_k is the position and v_k is the linear velocity of the magnet, m_k is the magnetic moment vector of the magnet and B_k is the additive bias field. The motion model in this case is linear and, using (2.4) and (2.6), is given by

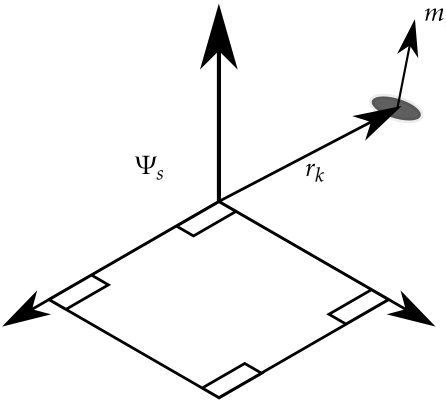

Figure 3.1: *The sensor network with defined frame and the magnet*

$$x_{k+1} = \underbrace{\begin{pmatrix} I & TI & 0 & 0 \\ 0 & I & 0 & 0 \\ 0 & 0 & I & 0 \\ 0 & 0 & 0 & I \end{pmatrix}}_{F} x_k + \underbrace{\begin{pmatrix} \frac{T^2}{2}I & 0 & 0 \\ TI & 0 & 0 \\ 0 & TI & 0 \\ 0 & 0 & TI \end{pmatrix}}_{G} \begin{pmatrix} w_k^v \\ w_k^m \\ w_k^B \end{pmatrix} \tag{3.4}$$

where T is the sampling time, $w_k^v \in N(0, Q^v)$, $w_k^m \in N(0, Q^m)$ and $w_k^B \in N(0, Q^B)$ are all uncorrelated and belonging to the linear velocity, magnetic moment and static field states respectively. If the sensor board is stationary the variance of the noise should be zero; or very close to zero for computational purposes.

For the case of a stationary sensor network the coordinate system of the sensor board, call it Ψ_s, can be seen as the world frame. The position of one of the magnetometers is defined as the origin and the position of the others are given related to this magnetometer. Let the position of the ith magnetometer in the coordinate system Ψ_s be θ_i. Using (3.2) the measurement model then becomes

$$y_k^i = \underbrace{B_k + J(r_k - \theta_i)m_k}_{h_i(x_k)} + e_k^i \quad i = 1 \ldots 4,\ e_k^i \in N(0, Q^i) \tag{3.5}$$

The measurement model is nonlinear so no analytical optimal filtering solution exists. Thus the extended Kalman filter given in Algorithm 2 is used. The dynamic model is already linear so

$$\frac{d(x_{k+1})}{dx_k} = F \tag{3.6}$$

For the Jacobian of the measurement function the following derivatives are needed see [Wahlström, 2013], as before let $\tilde{r}_k = r_k - \theta_i$

$$\frac{\partial h_i(x_k)}{\partial r_k} = \frac{3}{\|\tilde{r}_k\|^5}\left((\tilde{r}_k \cdot m_k)I + \tilde{r}_k m_k^T - \|\tilde{r}_k\| m_k^T + m_k \tilde{r}_k^T - 5\frac{(\tilde{r}_k \cdot m)}{\|\tilde{r}_k\|^2}\right) \tag{3.7a}$$

$$\frac{\partial h_i(x_k)}{\partial v_k} = 0 \tag{3.7b}$$

$$\frac{\partial h_i(x_k)}{\partial m_k} = J(r_k) \tag{3.7c}$$

$$\frac{\partial h_i(x_k)}{\partial B_k} = I \tag{3.7d}$$

The Jacobian for $h_i(x_k)$ is given by

$$\frac{\partial h_i(x_k)}{\partial x_k} = \begin{pmatrix} \frac{\partial h_i(x_k)}{\partial r_k} & \frac{\partial h_i(x_k)}{\partial v_k} & \frac{\partial h_i(x_k)}{\partial m_k} & \frac{\partial h_i(x_k)}{\partial B_k} \end{pmatrix} \tag{3.8}$$

Finally the Jacobian of the measurement function needed for Algorithm 2 is given by

$$h'(x_k) = \begin{pmatrix} \frac{\partial h_1(x_k)}{\partial x_k} \\ \frac{\partial h_2(x_k)}{\partial x_k} \\ \frac{\partial h_3(x_k)}{\partial x_k} \\ \frac{\partial h_4(x_k)}{\partial x_k} \end{pmatrix} \tag{3.9}$$

3.2 The Constrained Model

The relaxed model does not use all the information there is about the system. The norm of the magnetic moment of the permanent magnet is constant. The only change in the value of the moment vector m_k depends on the orientation of the magnet. Define a magnet frame Ψ_m where the z-axis is pointing in the direction of the moment vector. The magnetic moment vector in this frame is then given by

$$m^m = \|m\| \begin{pmatrix} 0 \\ 0 \\ 1 \end{pmatrix} \tag{3.10}$$

Using (2.10) the moment vector in the sensor frame is given by

$$m^s = R^{sm} m^m = \|m\| R^{sm} \begin{pmatrix} 0 \\ 0 \\ 1 \end{pmatrix} \tag{3.11}$$

where R^{sm} is the orientation of the m-frame with respect to the s-frame. Following the discussion in Section 2.4 this orientation is parametrized with a unit quaternion $q : \|q\| = 1$. The relation in (3.11) then becomes

$$m^s = \|m\| R^{sm}(q) \begin{pmatrix} 0 \\ 0 \\ 1 \end{pmatrix} \tag{3.12}$$

where $R^{sm}(q)$ is given by (2.12). The situation is illustrated in Figure 3.2. Note that for a stationary and level sensor network m^s is the same quantity as m in Section 3.1. The state vector used for this model is

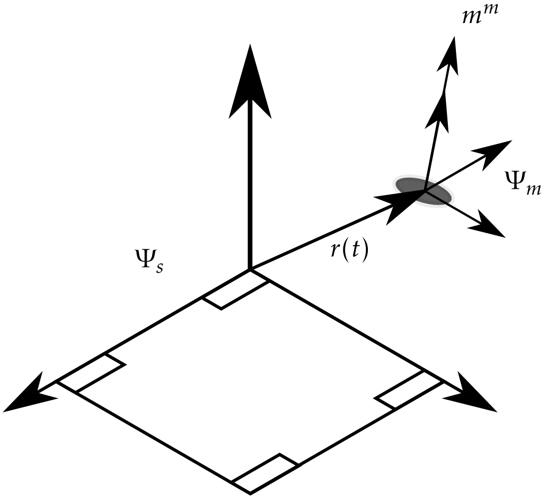

__Figure 3.2:__ The sensor network with defined sensor board frame and magnet frame

$$x(t) = \begin{pmatrix} r(t)^T & v(t)^T & B(t)^T & q(t)^T & \omega(t)^T \end{pmatrix}^T \tag{3.13}$$

where $r(t)$, $v(t)$ and $B(t)$ are the continuous counterparts to the states in (3.3), $q(t)$ is the quaternion describing the orientation of the magnet frame with respect to the sensor board frame and ω is the angular velocity of this orientation. Note that the states have to be continuous at this point so that (2.13a) can be used. Thus the continuous version of the constant velocity model, found in (2.3), has to be used on position and linear velocity, while the continuous random walk model, found in (2.5), is used on the static field vector $B(t)$ and the angular velocity ω. Collecting all these models in a continuous state space model finally yields

$$\dot{x} = \underbrace{\begin{pmatrix} 0 & I & 0 & 0 & 0 \\ 0 & 0 & 0 & 0 & 0 \\ 0 & 0 & 0 & 0 & 0 \\ 0 & 0 & 0 & \frac{1}{2}S(\omega) & 0 \\ 0 & 0 & 0 & 0 & 0 \end{pmatrix} x}_{f(x)} + \underbrace{\begin{pmatrix} 0 & 0 & 0 \\ I & 0 & 0 \\ 0 & I & 0 \\ 0 & 0 & 0 \\ 0 & 0 & I \end{pmatrix}}_{B} \underbrace{\begin{pmatrix} w^v(t) \\ w^B(t) \\ w^\omega(t) \end{pmatrix}}_{w} \tag{3.14}$$

where $w^v(t) \in N(0, Q^v)$, $w^B(t) \in N(0, Q^B)$ and $w^w(t) \in N(0, Q^w)$ are all uncorrelated. Note that the input noise matrix B should not be confused with the bias magnetic field state $B(t)$.

This model is nonlinear and continuous so to use it in a computer implemented filter it needs to be discretized and linearized. Optimally the discretization should be done first. This can only be done if there exists a solution to the sampling problem, discussed in Section 2.1, however, and to the best of the authors knowledge such a solution does not exist for this model. Thus the model is linearized and then discretized. The problem with this is that the linearization error is propagated in the state update as well as the covariance matrix update. For a discussion on this see [Gustafsson and Isaksson, 1996].

Using (2.13) the following derivatives can be found

$$\frac{\partial \dot{q}}{\partial q} = \frac{1}{2} S(\omega) \tag{3.15}$$

$$\frac{\partial \dot{q}}{\partial \omega} = \frac{1}{2} \bar{S}(q) \tag{3.16}$$

Using this, and the fact that the linear part of the Jacobian is not affected by differentiation, the Jacobian of $f(\,)$ is found to be

$$f'(\hat{x}) = \begin{pmatrix} 0 & I & 0 & 0 & 0 \\ 0 & 0 & 0 & 0 & 0 \\ 0 & 0 & 0 & 0 & 0 \\ 0 & 0 & 0 & \frac{1}{2}S(\hat{\omega}) & \frac{1}{2}\bar{S}(\hat{q}) \\ 0 & 0 & 0 & 0 & 0 \end{pmatrix} \tag{3.17}$$

A first order Taylor expansion of (3.14) around some estimate gives the linearized model

$$\dot{x} \approx f(\hat{x}) + f'(\hat{x})(x - \hat{x}) + Bw = \underbrace{f'(\hat{x})}_{F}\, x + \underbrace{f(\hat{x}) - f'(\hat{x})\hat{x}}_{u} + Bw(t) \tag{3.18}$$

The constant part is treated as a known system input and is given by

$$u = f(\hat{x}) - f'(\hat{x})\hat{x} = \begin{pmatrix} 0 \\ 0 \\ 0 \\ 0 \\ \frac{1}{2}\bar{S}(\hat{q})\hat{\omega} \end{pmatrix} \tag{3.19}$$

The discrete model is now given by following the discretization procedure in Section 2.1

$$x_{k+1} = F_k x_k + \tilde{G}_k u + G_k w_k, \quad w_k \in N(0, Q) \tag{3.20}$$

where

$$F_k = \exp\left(f'(\hat{x})T\right) \tag{3.21}$$

$$\tilde{G}_k = \int_0^T \exp\left(f'(\hat{x})\tau\right) d\tau \tag{3.22}$$

and

$$G = \tilde{G}_k B \tag{3.23}$$

The matrices F_k and $\tilde{G}_k$ can be computed conveniently by using the fact that

$$\exp\begin{pmatrix} f'(\hat{x})T & IT \\ 0 & 0 \end{pmatrix} = \begin{pmatrix} F_k & \tilde{G}_k \\ 0 & I \end{pmatrix} \tag{3.24}$$

The linearization is done in the Kalman filter loop so $\hat{x} = \hat{x}_{k|k}$. Let as before θ_i be the position of the ith sensor in the coordinate frame Ψ_s. Let $q_k = q$ for convenience. Considering the relation given in (3.12), and using (2.12), a measurement at time k is given by

$$y_k^i = B_k + J(r_k - \theta_i)R^{sm}(q)\|m\| \begin{pmatrix} 0 \\ 0 \\ 1 \end{pmatrix} + e_k^i = \tag{3.25}$$

$$= B_k + \|m\| J(r_k - \theta_i) \underbrace{\begin{pmatrix} 2q_1q_3 - 2q_0q_2 \\ 2q_2q_3 + 2q_0q_1 \\ q_0^2 - q_1^2 - q_2^2 + q_3^2 \end{pmatrix}}_{D} = \tag{3.26}$$

$$= \underbrace{B_k + \|m\| J(r_k - \theta_i) D}_{h_i(x_k)} + e_k^i, \ i = 1 \dots 4 \quad e_k^i \in N(0, R^i) \tag{3.27}$$

where e_k is uncorrelated with w_k. The Jacobian of the measurement function with respect to position r_k is essentially the same as in (3.7a) if m_k is substituted with D. The derivative of h_i with respect to ω is obviously zero. The derivative of $h_i(x_k)$ with respect to the quaternion is given by

$$\frac{\partial h_i(x_k)}{\partial q} = J(r_k - \theta_i) \begin{pmatrix} -2q_2 & 2q_3 & -2q_0 & 2q_1 \\ 2q_1 & 2q_0 & 2q_3 & 2q_2 \\ 2q_0 & -2q_1 & -2q_2 & 2q_3 \end{pmatrix} \tag{3.28}$$

The Jacobian to be used in Algorithm 2 can now be constructed analogously to (3.8) and (3.9).

To represent a rotation the quaternion must be a unit quaternion as noted in Section 2.4. This constraint is included as a hard constraint in the measurement update so that

$$q_{k|k}^f = \frac{q_{k|k}^f}{\|q_{k|k}^f\|} \tag{3.29}$$

where $q_{k|k}^f$ is the filter estimate of the quaternion. The constraint can also be implemented as a soft constraint using an additional measurement equation

$$q^* = \|q\|^2 + e_i^*, \quad e_i^* \in N(0, \mathrm{diag}(r)) \tag{3.30}$$

The pseudo measurement $q^* = 1$ is then used. The good thing about this is that the constraint is included in the covariance update, the bad thing is that the constraint is not guaranteed at all times.

3.3 Toward a Non Stationary Sensor Network

The models in the past sections have all assumed a stationary sensor network, so that the sensor frame Ψ_s aligned with the world frame Ψ_w. Relation (3.2) is only valid if this assumption is correct. If this assumption is not correct the sensor i

will at time k measure a rotated field

$$y_k^i = R^{sw}\left(B + J(r_{k,i}^w)R^{wm}\begin{pmatrix}0\\0\\\|m\|\end{pmatrix}\right) + e_k^i, \quad e_k^i \in N(0, R^i) \tag{3.31}$$

where $r_{k,i} = r_k - \theta_i$. To proceed the following lemma is needed

3.2 Lemma. *Given two coordinate frames Ψ_a and Ψ_b sharing origin, and the rotation matrix R_{ab} between the two frames, the following holds:*

$$J(r^a)R_{ab} = R_{ab}J(r^b) \tag{3.32}$$

Proof: The rotation matrix R_{ab} is orthogonal, i.e. it satisfies

$$R_{ab}^T R_{ab} = I_3 \tag{3.33}$$

The rotation matrix will therefore also preserve norms. The position vector can be transformed between the frames according to $R_{ab}r^b = r^a$. Using these relations the left hand side of equation 3.32 can be rewritten as

$$\begin{aligned}
J(r^a)R_{ab} &= J(R_{ab}r^b)R_{ab} = \{\text{isometric transformations preserve norms}\} = \\
&= \frac{1}{\|r^b\|^5}\left(3R_{ab}r^b\left(R_{ab}r^b\right)^T - \|r^b\|^2 I_3\right)R_{ab} \\
&= \frac{1}{\|r^b\|^5}\left(3R_{ab}r^b(r^b)^T R_{ab}^T R_{ab} - \|r^b\|^2 R_{ab}\right) = \{\text{equation 3.33}\} = \\
&= R_{ab}\frac{1}{\|r^b\|^5}\left(3r^b(r^b)^T - \|r^b\|^2 I_3\right) = R_{ab}J\left(r^b\right)
\end{aligned}$$

□

Now (3.31) can be manipulated as follows

$$y_k^i = R^{sw}\left(B^w + J(r_{k,i}^w)R^{wm}\begin{pmatrix}0\\0\\\|m\|\end{pmatrix}\right) + e_k^i = \{\tilde{B} = R^{sw}B^w\} = \tag{3.34}$$

$$= \tilde{B} + R^{sw}J(r_{k,i}^w)R^{wm}\begin{pmatrix}0\\0\\\|m\|\end{pmatrix} + e_k^i = \{\text{Lemma 3.2}\} = \tag{3.35}$$

$$= \tilde{B} + J(r_{k,i}^s)R^{sw}R^{wm}\begin{pmatrix}0\\0\\\|m\|\end{pmatrix} + e_k^i = \tag{3.36}$$

$$= \tilde{B} + J(r_{k,i}^s)R^{sm}\begin{pmatrix}0\\0\\\|m\|\end{pmatrix} + e_k^i, \quad e_k^i \in N(0, R^i) \tag{3.37}$$

where the well-known relation $R^{sw}R^{wm} = R^{sm}$ has been used. Equation (3.37) implies that the models in Section 3.1 and 3.2 can be used in the non stationary case, but the orientation and position of the magnet will then be given relative the moving sensor board frame.

For a non stationary network $\tilde{B}_k$ is used in the state vector instead of B_k. Unlike B_k the state $\tilde{B}_k$ is time-varying since the static field is measured from different orientations when the sensor board is moving around. This means that the system noise input must have a larger covariance compared to the state B_k for the stationary network so that $\tilde{B}_k$ is allowed to change.

4

Calibration

The models developed in Chapter 3 assumes that the bias field B is exactly the same viewed from the different magnetometers. Normally the magnetometers will measure different values for the field due to various imperfections in the sensing. There are numerous reasons for why the magnetometers would give different values of the same measured quantity. Therefore it is imperative that the magnetometers are calibrated before the measurements are used. In this work several different anomalies in the sensor measurements will be corrected for.

Errors in the sensor readings The sensors can have physical errors that are specific to each sensor. These errors include

- Non-orthogonality of the sensor axes
- Differences in sensitivity between the sensor axes
- Zero bias in the sensor readings.

Gain errors between the sensors The sensors could have a difference in gain reading with respect to each other for various reasons.

Difference in orientation of the sensor frames The measurement models only make sense if the orientation of the sensor frames are aligned.

4.1 Gain and Sensor Reading Errors

The problem of calibrating for gain and sensor errors are treated extensively in [Hol, 2011] and [Kok et al., 2012]. The calibration for the magnetometers in this work basically follows the calibration in [Kok et al., 2012] up until the involvement of alignment between magnetometer and accelerometer frames.

If the sensor board is rotated without any permanent magnets present the measured magnetic moment from one of the sensors given in the sensor frame, m^s, should be related to the magnetic moment in the world frame, call it m^w, as

$$m^s = R^{sw} m^w \tag{4.1}$$

A data set measured from a rotated sensor network should be given by $\{y^s_{m,k}\}_{k=1}^K = \{m^s_k\}_{k=1}^K$. If this is indeed the case equation (4.1) implies that this data set is lying on a sphere with a radius of the norm of the magnetic moment in the w-frame. Errors in gain and sensor readings can be modelled as an affine transformation of the magnetic moment:

$$y^s_k = Dm^b_k + o + e_k \tag{4.2}$$

where $D \in \mathbb{R}^{3\times3}$ and the noise $e^k \in N(0, R)$ is included for the sake of completeness. This means that the measurements from the rotated sensor platform will be situated on an ellipse instead of a sphere. The calibration procedure consist of finding an estimate of $\{D, o\}$ and doing the inverse affine transformation on the measurements. This is done by finding the optimal mapping from the ellipse to the aforementioned sphere using a least-squares method. For further details consult [Kok et al., 2012] and [Hol, 2011].

4.2 Frame Differences

If measurement noise is not considered any differences that possibly still exist between the readings of the sensors can be modelled as a general transformation between the measurements from the various sensors, and the difference in orientation between the sensors can be modelled as a rotation between the measured values, i.e. the values from the jth sensor can be written in terms of the values of the ith sensor according to

$$y_j = \tilde{D}R^{ji} y_i \triangleq G^{ji} y_i \tag{4.3}$$

Consider the transformation from the ith sensor to the first sensor. Let the 9 parameters in the G^{1i} matrix be represented by the vector θ_i. Using the well-known formula

$$\text{vec(ABC)} = (C^T \otimes A)\,\text{vec(B)} \tag{4.4}$$

equation (4.3) for $i = 1$ can be written

$$\begin{aligned} y_1 &= G^{1i} y_i = IG^{1i} y_i = \{\text{vec operator does not change vectors}\} = && (4.5)\\ &= \text{vec}(\mathrm{IG^{1i}y_i}) = \{\text{equation } 4.4\} = (y_i^T \otimes I_3)\,\text{vec}(\mathrm{G^{1i}}) = (y_i^T \otimes I_3)\theta_i && (4.6)\end{aligned}$$

For k samples consider the matrices of samples

$$Y_1 = \begin{pmatrix} y^1_1 & \cdots & y^1_k \end{pmatrix}$$
$$Y_i = \begin{pmatrix} y^i_1 & \cdots & y^i_k \end{pmatrix}$$

Using these matrices the relation corresponding to (4.6) for k samples can be written

$$\mathrm{vec}(\mathrm{Y}_1) = \underbrace{(Y_i^T \otimes I_3)}_{H} \theta_i$$

and the parameters of the transformation matrix can be found using the normal equations

$$\theta_i = (H^T H)^{-1} H^T \,\mathrm{vec}(\mathrm{Y}_1)$$

normally solved using matrix factorization methods. After the matrices G^{1i} has been acquired all data sets can be transformed to the frame orientation of the first sensor by transforming the data with the inverse operators. An example of measurement data prior to calibration can be found in Figure 4.1. The same data after calibration is shown in Figure 4.2. Note that especially sensor 3 has a null shift prior to calibration. This null shift is gone after the calibration.

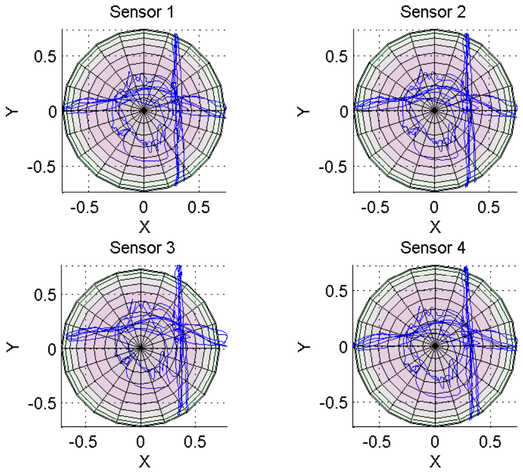

Figure 4.1: *Projection to the xy-plane of measurement data with a rotated sensor board without a magnet present prior to calibration*

4.3 Position Calibration

For a good filter performance it is important to have the positions of the sensors in the sensor frame with good accuracy. The magnetometers used for the measurements in this work are just one component of an inertial measurement unit, i.e. they come bundled with a gyro and an accelerometer. The gyro measure angular velocity, usually with some bias, while the accelerometer measure the linear acceleration. In this work these measurements are only used to calibrate for sensor positions. Consider two of the sensors with measurement frames Ψ_{s1} and Ψ_{s2}

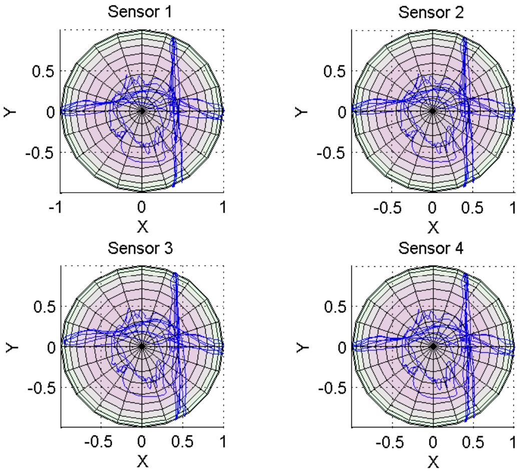

Figure 4.2: *Projection to the xy-plane of measurement data with a rotated sensor board without a magnet present after calibration*

respectively. The two sensors are fixed on the sensor board, i.e. they are placed on a rigid body. Let ω and α be the angular velocity and angular acceleration of the rigid body. Furthermore let a_{s1} and a_{s2} be the linear acceleration of the two sensors, R^{s1s2} the rotation matrix between the two frames as usual and r the relative position of the sensors. Calibrating for the relative position between the two sensors can then be done by using the formula for acceleration of two points fixed on a rigid body

$$a_{s1} = R^{s1s2}a_{s2} + R^{s1s2}\left((\omega) \times (\omega \times r)\right) + \alpha \times r \tag{4.7}$$

The quantities a_{s1} and a_{s2} are measured by the accelerometer of the respective sensor while ω is measured by the gyro of both sensors. Numerical differentiation of ω gives α and then p and R^{s1s2} can be solved for using for example a Gauss-Newton algorithm. This procedure can be repeated to get the relative position from one of the sensors with respect to all the others. The position of this sensor can then be treated as the origin in the sensor network. Note that the possible gyro bias has to be accounted for beforehand and that (4.7) assumes that the accelerometer and the gyro of the sensors share origin.

4.4 Magnetic Moment Norm

To use the model developed in Section 3.2 the value of the norm of the magnetic moment of the permanent magnet is needed. In some cases this value is tabulated and thus easily obtainable, but in other cases it needs to be measured from the magnet. One way of acquiring the value of the magnetic moment norm is to use a modified version of the model detailed in Section 3.2 where as many DoF as possible are removed. To this end an experiment was performed where the magnet was moved around on a table to remove one DoF in the z-direction and two DoF for the orientation. The height variable was still included as a state but with a very small noise input variance, in the order of the machine constant. The magnet was positioned on the table so that the magnetic moment norm, and thus the z-axis of the magnet frame, was pointing upwards. Therefore the substitution $R^{sm}(q) = I$ could be made in (3.25). Also the bias field was measured individually for each sensor and then subtracted from the measurements with the magnet present eliminating the need for the bias state and sensor calibration. Considering all this and using random walk, with a very small input noise covariance, on the magnetic moment norm $\|m\|$ the following 7-dimensional state vector was used

$$x_k = \begin{pmatrix} r_k^T & v_k^T & \|m\| \end{pmatrix}^T \tag{4.8}$$

along with the state space model

$$x_{k+1} = \begin{pmatrix} I & TI & 0 \\ 0 & I & 0 \\ 0 & 0 & 1 \end{pmatrix} x_k + \begin{pmatrix} \frac{T^2}{2}I & 0 \\ TI & 0 \\ 0 & T \end{pmatrix} \begin{pmatrix} w_k^v \\ w_k^m \end{pmatrix} \tag{4.9}$$

$$y_k^i = \|m\| J(r_k - \theta_i) \begin{pmatrix} 0 \\ 0 \\ 1 \end{pmatrix} + e_k^i, \quad e_k^i \in N(0, R^i) \tag{4.10}$$

where as usual $w_k^v \in N(0, Q^v)$, $w_k^m \in N(0, Q^m)$ and e_k^i are uncorrelated.

4.5 Sensor Covariance Estimation

The noise distribution e_k^i of the sensors is assumed to be zero mean white Gaussian noise and therefore fully described by its covariance matrix, i.e. $e_k^i \in N(0, R^i)$. The covariance matrix of the ith sensor can be estimated from measurements $\{y_k^i\}_{k=1}^K$ done without any magnet present by the sample covariance

$$\hat{R}^i = \frac{1}{K-1} \sum_{k=1}^{K} \left(y_k^i - \bar{y}^i\right)\left(y_k^i - \bar{y}^i\right)^T$$

$$\bar{y}^i = \frac{1}{K} \sum_{k=1}^{K} y_k^i$$

This was done for each experiment since the same 4 sensors were not always used. One of the estimated covariance matrices is given in (4.11).

$$10^{-5}\begin{pmatrix} 0.2051 & -0.0215 & 0.0064 & 0.0419 & -0.0129 & 0.0223 & 0.0387 & -0.0158 & 0.0270 & 0.0471 & -0.0158 & 0.0178 \\ -0.0215 & 0.1440 & -0.0036 & -0.0130 & 0.0162 & -0.0014 & -0.0142 & 0.0207 & -0.0077 & -0.0116 & 0.0156 & -0.0056 \\ 0.0064 & -0.0036 & 0.2928 & 0.0220 & 0.0026 & 0.0234 & 0.0306 & 0.0000 & 0.0071 & 0.0176 & 0.0003 & 0.0206 \\ 0.0419 & -0.0130 & 0.0220 & 0.1989 & -0.0171 & 0.0021 & 0.0388 & -0.0142 & 0.0279 & 0.0453 & -0.0126 & 0.0195 \\ -0.0129 & 0.0162 & 0.0026 & -0.0171 & 0.1473 & -0.0026 & -0.0139 & 0.0170 & -0.0087 & -0.0139 & 0.0086 & -0.0034 \\ 0.0223 & -0.0014 & 0.0234 & 0.0021 & -0.0026 & 0.4886 & 0.0274 & 0.0067 & 0.0264 & 0.0277 & -0.0091 & 0.0204 \\ 0.0387 & -0.0142 & 0.0306 & 0.0388 & -0.0139 & 0.0274 & 0.1967 & -0.0244 & -0.0019 & 0.0383 & -0.0128 & 0.0169 \\ -0.0158 & 0.0207 & 0.0000 & -0.0142 & 0.0170 & 0.0067 & -0.0244 & 0.1649 & -0.0183 & -0.0159 & 0.0124 & 0.0001 \\ 0.0270 & -0.0077 & 0.0071 & 0.0279 & -0.0087 & 0.0264 & -0.0019 & -0.0183 & 0.4226 & 0.0241 & -0.0045 & 0.0082 \\ 0.0471 & -0.0116 & 0.0176 & 0.0453 & -0.0139 & 0.0277 & 0.0383 & -0.0159 & 0.0241 & 0.2223 & -0.0200 & -0.0012 \\ -0.0158 & 0.0156 & 0.0003 & -0.0126 & 0.0086 & -0.0091 & -0.0128 & 0.0124 & -0.0045 & -0.0200 & 0.1489 & -0.0096 \\ 0.0178 & -0.0056 & 0.0206 & 0.0195 & -0.0034 & 0.0204 & 0.0169 & 0.0001 & 0.0082 & -0.0012 & -0.0096 & 0.3063 \end{pmatrix} \tag{4.11}$$

5

Validation

When designing a pose estimation system meant for practical use it is imperative to have a measure of the accuracy and performance of the system. To get such a measure ground truth data is needed, i.e. the actual correct position and orientation of the target, in this case the permanent magnet. Ground truth measurements can be acquired using an optical 3D-image system such as the visualEyez system shown in Figure 5.1. This chapter will show the results from such a ground truth experiment and also give a detailed explanation of how the data was gathered and processed.

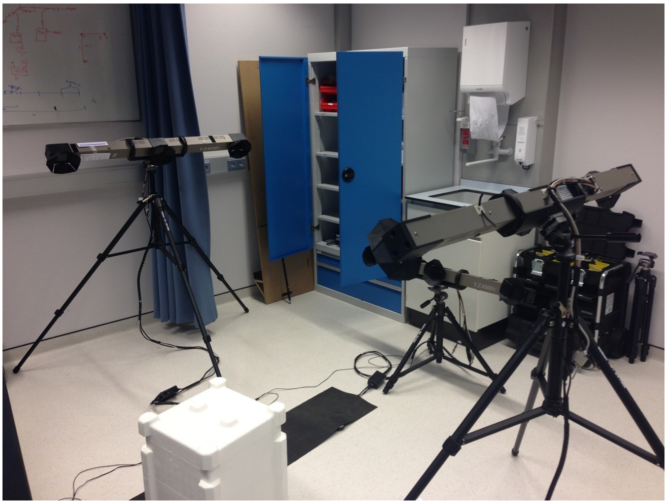

Figure 5.1: *Three visualEyez system cameras*

5.1 Acquiring Ground Truth Measurements

The visualEyez system consists of one or multiple 3D-cameras sensing light-emitting led markers. The system tracks the position of the led markers. By having three or more markers a frame can be constructed, where subtracted position measurements become basis vectors in the frame. The experiment is performed by putting the magnet on a separate board. The markers are placed on this board so that they define a frame for the board. Call this frame of the magnet board Ψ_{mb}. Markers are also placed on the sensor board such that another frame is defined, call this frame of the sensor board Ψ_{sb}. The situation is illustrated in Figure 5.2. The position estimates from the visualEyez system is given in the frame of the cameras. Consider the situation in Figure 5.3. The various quantities one immediately gets from the visualEyez system is summarized in Table 5.1 The estimate given by the magnetic tracking system is the position of the magnet in the sensor-

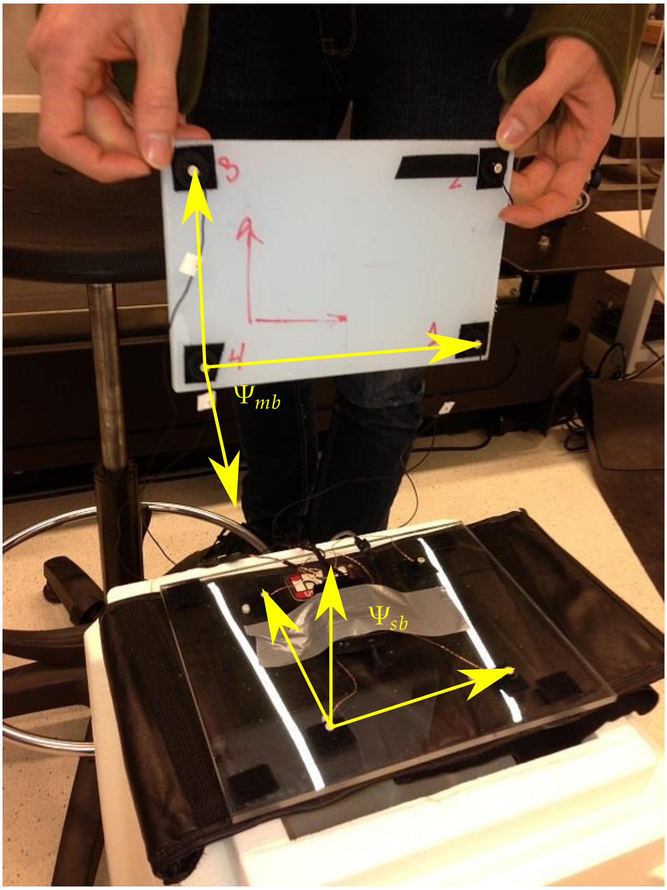

Figure 5.2: *The magnet-board and sensor board with markers and corresponding frames defined*

p_{mb}^{cam}	Position of the magnet-board given in the camera frame
p_{sb}^{cam}	Position of the sensor board given in the camera frame
R^{cammb}	Orientation of the magnet-board frame with respect to the camera frame
R^{camsb}	Orientation of the sensor board frame with respect to the camera frame

Table 5.1: *Data given by the visual system*

frame p_m^s. Given that the position of the magnet in the frame of the magnet board, p_m^{mb}, and that the position of the origin of the sensor frame Ψ_s in the frame of the sensor board, p_s^{sb} are both known vectors, the position of the magnet and the sensors are given by

$$p_m^{cam} = p_{mb}^{cam} + R^{cammb} p_m^{mb}$$

and

$$p_s^{cam} = p_{sb}^{cam} + R^{camsb} p_s^{sb}$$

respectively. The position of the magnet in the sensor frame can now be acquired by

$$p_m^s = R^{ssb} \left((R^{camsb})^T (p_m^{cam} - p_s^{cam}) \right)$$

The three cameras were calibrated with respect to each other using a calibration device and proprietary software.

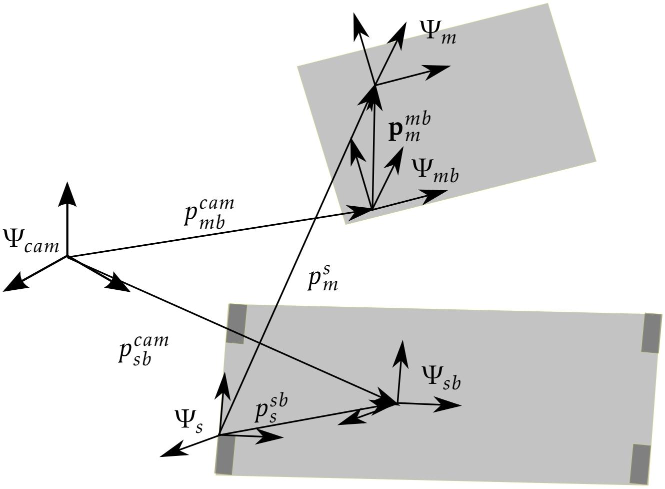

Figure 5.3: *The various frames involved in the experiment*

5.2 Tracking Comparison for the Relaxed Model

An extended Kalman filter was used together with the relaxed model outlined in Section 3.1 to estimate the magnet trajectory. The same trajectory was simultaneously measured by the visualEyez system. The results of this validation experiment is shown in Figure 5.4, 5.5 and 5.6 respectively. Note that the sampling time is $T = \frac{1}{75}$ $[s]$.

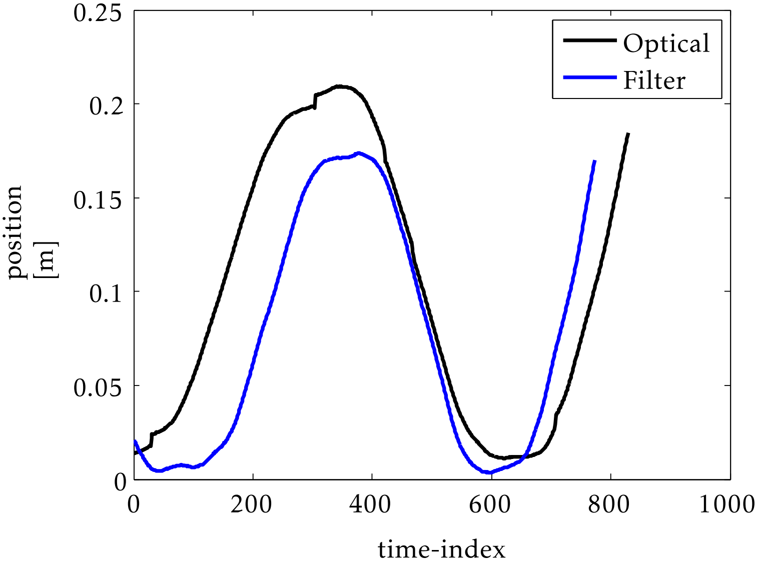

Figure 5.4: x-component of magnet trajectory using an extended Kalman filter and the relaxed model

For comparison the same magnet trajectory was also estimated using a simpler model where the bias field was measured prior to deploying the magnet and then subsequently subtracted from the measurements with the magnet present. This was done individually for each sensor so the assumption that the field has to be the same for all sensors was no longer needed. Since the magnetic calibration routines mostly were designed to ensure the assumption of the same bias field for all sensors the calibration was not used in this case. The result for this estimation, also done using an extended Kalman filter, is shown in Figure 5.7, 5.8 and 5.9.

5.3 Proof of Concept for the Constrained Model

The constrained model is more sensitive to the accuracy of the initial guesses and the quality of the measurements, a possible explanation to this is given in Section 5.4. Unfortunately due to the complexity of acquiring both magnetic measurements and optical measurements simultaneously, and also due to restricted lab access and time constraints, no ground truth experimental data was measured

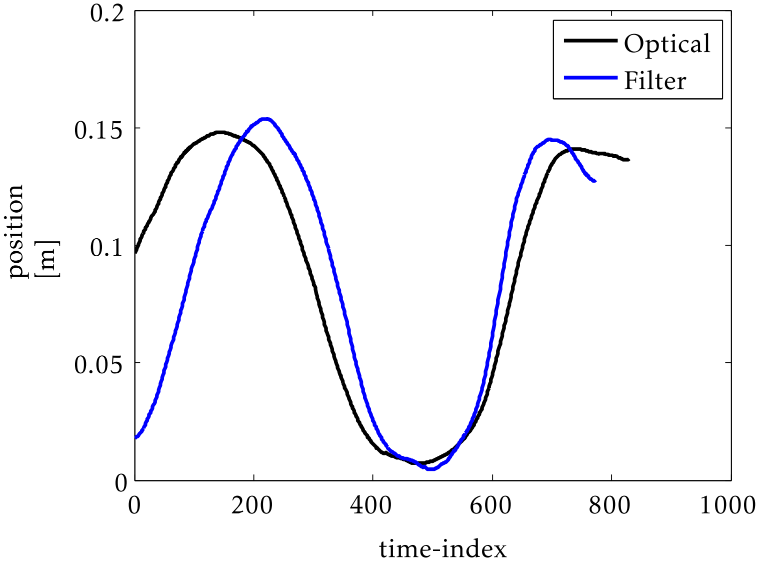

Figure 5.5: *y-component of magnet trajectory using an extended Kalman filter and the relaxed model*

that the constrained model was able to reconstruct. The magnet trajectory reconstruction for the constrained model diverges using the data set in Section 5.2. As a proof of concept for the model a reconstruction of the data used to estimate the magnetic moment norm is provided. This experiment, discussed in Section 4.4, was controlled more diligently and initial guesses close to the actual ones are given to the filter. The positions estimates of the magnet can be found in Figure 5.10, 5.11 and 5.12 respectively, while a 3D-image of the reconstruction along with the reconstructed orientation of the magnet is shown in Figure 5.13. Some points on the trajectory and the orientation of the magnet frame with respect to the sensor board frame at those points are shown in the image. The magnet was moved around approximately like the trajectory shows. Also note that the magnet was sliding on a table in this experiment so the z-direction of the magnet frame was always pointing upwards. This is indeed the case in the reconstruction as well. Also note that the other two principal axes wander randomly. This is due to the unobservability of the rotation around the magnets own axis discussed in Chapter 3.

5.4 Discussion

As noted in Section 2.3 the extended Kalman filter is a more or less ad hoc solution to the nonlinear filtering problem. It has worked remarkably well in many applications but there is no guarantee that it will work for all cases. For the linear filtering problem however the Kalman filter indeed gives an optimal unbiased

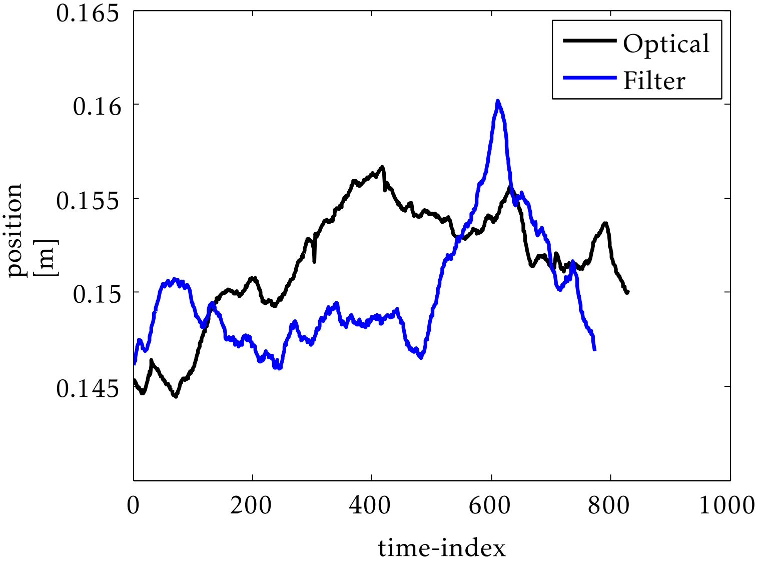

Figure 5.6: *z-component of magnet trajectory using an extended Kalman filter and the relaxed model*

solution to the estimation problem in the minimum variance sense. An interpretation is that the Kalman filter is a solution to the a convex optimization problem and thus a global solution, see [Schon et al., 2003]. A reasonable idea is that the more nonlinear a problem is the more nonconvex it becomes making it harder to find the correct solution. The relaxed model has gotten its name from the fact that not all information about the system is included. It lacks the constraint that the magnetic moment vector should always be on a sphere with the radius being the constant magnetic moment vector norm. The model does include all vectors in this sphere as a possible solution, but it does not force the moment vector to satisfy the constraint. Thus it can be interpreted as a relaxation of the physical situation giving a more convex problem in that the dynamic model now is linear. A more linear model is less sensitive to perturbations in measuring conditions and to the accuracy of input noise magnitudes and starting guesses. The fully constrained model developed in Section 3.2 is indeed more sensitive and more prone to divergence than the relaxed model. It works in many cases but a slight change in initial guess or input noise can make it diverge. An additional explanation for this behaviour of the constrained model could be that one of the angles is unobservable. This angle is included in the quaternion state and wanders erratically. The erratic behaviour of the unobserved angle is also propagated to the angular rate state.

The results from the ground truth experiments were not satisfactory. It seems like there is a bias and a time shift between the filter trajectory estimation and the estimate from the optical system. The poor performance is even more surprising considering that a model closely related to the one used in Figure 5.7, 5.8 and 5.7,

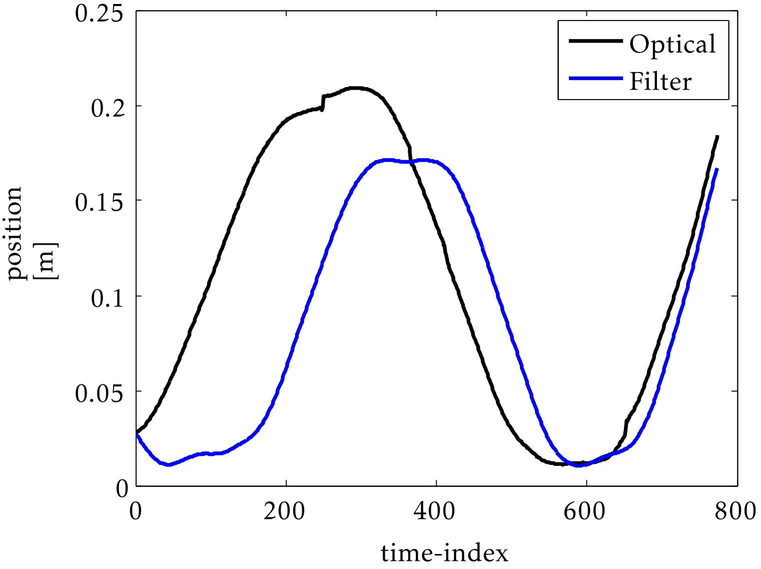

Figure 5.7: *x-component of magnet trajectory using an extended Kalman filter and simplified model without bias state*

where the bias state is not included and the bias field is measured separately by all the sensors and subsequently removed from the measurements with the magnet present, has been tested before by the sensor fusion group in Linköping and the results were much more accurate than here. How can this be? Well, firstly the sensors were different. In this work xsens MTw inertial measurement units were used. These include a gyro, an accelerometer and a magnetometer. For the usual orientation estimation approach done by IMUs the magnetometer is perhaps the least vital component so the magnetometer is possibly not the component of the highest quality.

The exact position of the magnetometer inside the MTw shown in Figure 1.1 is unknown. This is not crucial to filter performance since the exact position of the accelerometer is known due to the position calibration detailed in Section 4.3 and it can be assumed that the relative position of the accelerometer and the magnetometer is the same for all sensors. A translation of sensor positions does not affect filter performance since it is the relative position between the sensors that define the sensor coordinate frame. The exact position of the magnetometer is crucial when a ground truth comparison is to be made however since the coordinate frames of the reference system has to be aligned with the filter coordinate frame.

In an experiment done where the static magnetic field was measured at the same location by the sensors used it was found that some of the sensors had a large nullshift. This could possibly be explained by the fact that the MTw's can be calibrated for a disturbed magnetic environment such that the calibration is hard

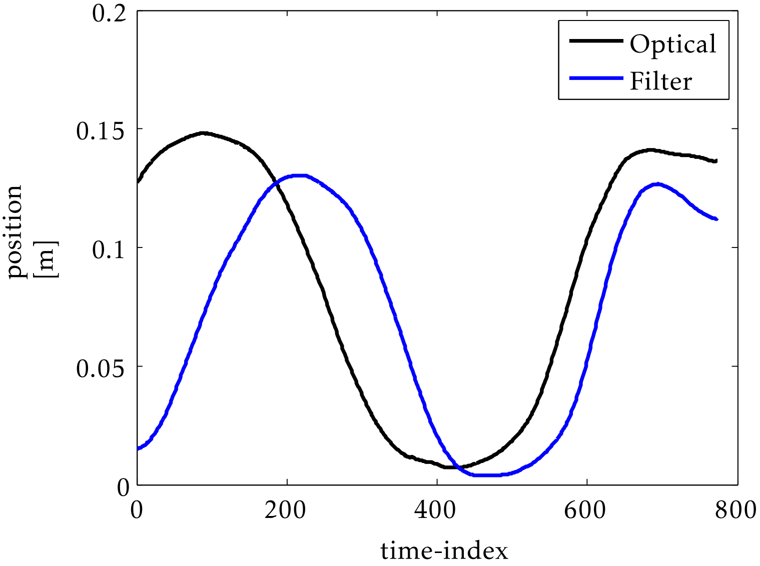

Figure 5.8: *y-component of magnet trajectory using an extended Kalman filter and simplified model without bias state*

coded into the firmware. This calibration could at the time of this work not be reset due to limitations in the proprietary software. This was fixed just as the project was over. There is also a small problem with the sensors causing the battery to act as an actuated magnet when MTw's are used wirelessly. The extent of this problem is not known so it is unclear how it could have affected the filter estimate.

Errors in the comparison arise also due to the difficulty of getting the LEDs exactly aligned with the sensors and the magnet. Furthermore, even given an optimal measuring situation, there is of course an uncertainty in the optical system position estimation. This uncertainty should be very small however.

A problem with optical systems, noted in Chapter 1, is that they need line of sight at all times to the target. To ensure this one can use multiple cameras. The cameras have to be calibrated toward each other however and it was difficult to get a good calibration. Often the position estimates suddenly jumped several centimetres when the cameras switched. Also, even with several cameras it is not guaranteed that there always is clear line of sight. For some of the LED marker measurements in the ground truth experiment as many as 20 % of the samples were missing. The missing values are given by interpolation increasing the uncertainty in the estimate.

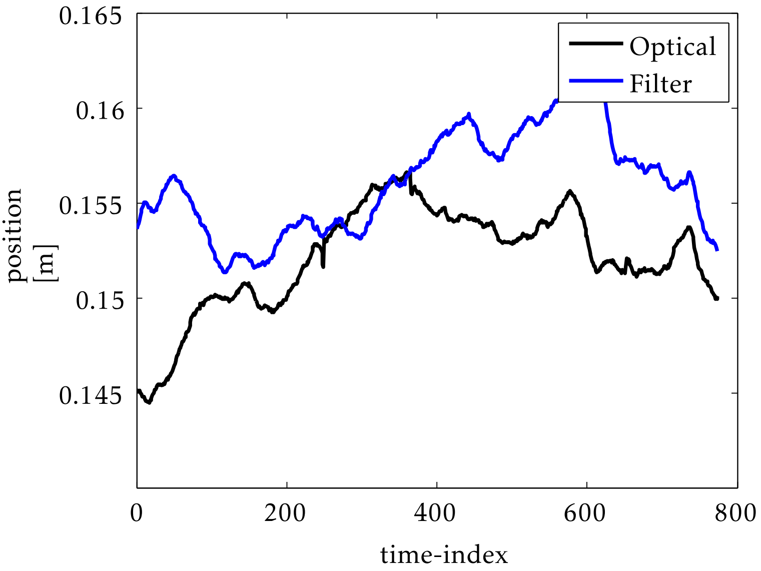

Figure 5.9: *z-component of magnet trajectory using an extended Kalman filter and simplified model without bias state*

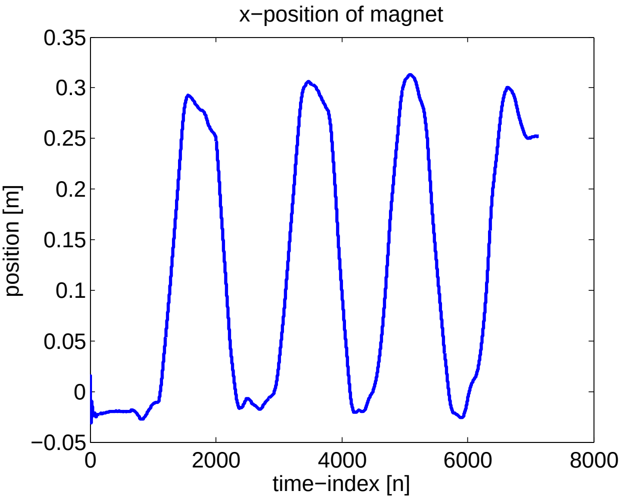

Figure 5.10: *x-component of the sliding magnet experiment, reconstructed by the constrained model*

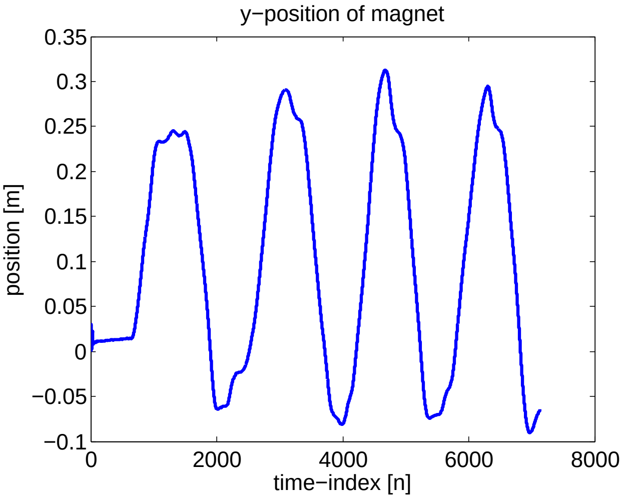

Figure 5.11: *y-component of the sliding magnet experiment, reconstructed by the constrained model*

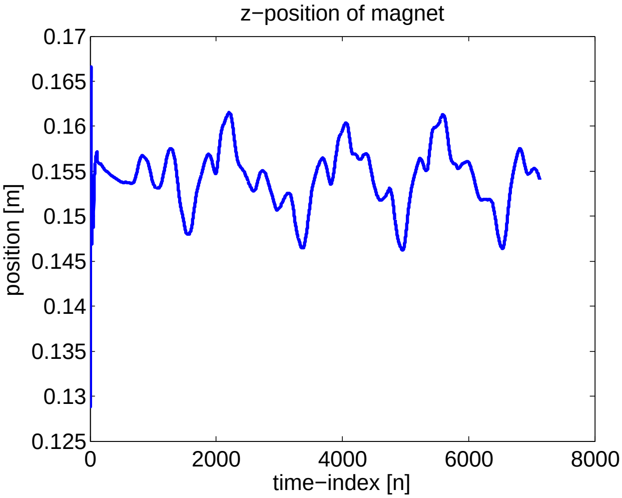

Figure 5.12: *z-component of the sliding magnet experiment, reconstructed by the constrained model*

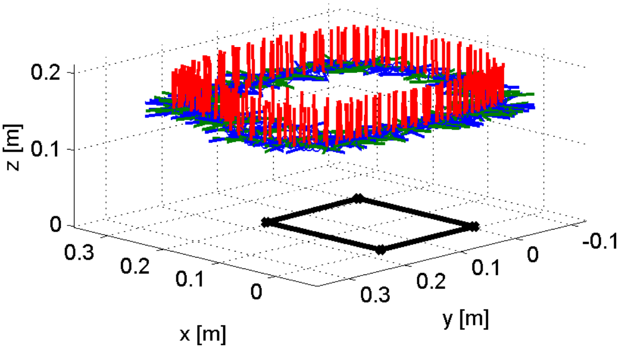

Figure 5.13: *Position and orientation estimates of the sliding magnet experiment by the constrained model. Note that the x-axis of the magnet frame orientation at a certain point is shown in blue, the y-axis is shown in green and the z-axis is shown in red*

6

Conclusions

A system for drift free pose estimation has been created. This was done using a network of magnetometers sensing the magnetic field of a permanent magnet. The system estimates the position and orientation of the magnet with respect to the sensor network. A small neodymium super magnet can be used to have a tracking volume with a radius of about half a metre per sensor. The magnet can be placed at locations whose position and orientation is of interest, for example a human limb for motion tracking. Two models have been developed for the purpose of pose estimation of the magnet. Both model the magnetic field from the magnet as a field from a magnetic dipole. One of the models parametrizes the orientation of the magnet with the dipole moment vector and does not use the fact that the norm of this vector should be constant. Call this model the relaxed model. The other model include the constraint on the magnetic dipole moment vector and parametrizes the orientation using quaternions; this model also includes the angular rate as a state. Call this model the constrained model. The dipole field is invariant to rotation around its own axis. Therefore the constrained model includes an unobservable angle in the state. The constrained model is also nonlinear both in the measurement equation and the dynamic equation while the relaxed model is nonlinear only in the measurement equation.

Several calibration routines have been developed for the sensor network. The field measured by the sensors is a superposition of the earth's magnetic field, possibly disturbed by metallic fixtures in the local environment, and the dipole field. An assumption for both models is that the measured earth's magnetic field is the same for all sensors. It was especially to ensure this assumption that calibration was necessary.

Pose estimation was done using an extended Kalman filter. The models were tested by comparing their reconstruction of the magnet trajectory with the reconstruction of the magnet trajectory from an optical reference system. The reconstruction for the data set measured during this experiment could not be reconstructed with the constrained model, possibly due to the larger nonlinearity of this model compared to the relaxed model or the effects of the unobservability of one of the angles. The reconstruction of the data set could be done with the relaxed model. The comparison between this trajectory and the trajectory estimated by the reference system shows that further improvements can be done, both for the model and the experimental setup. A magnet trajectory from a different more controlled experiment where some degrees of freedom have been removed is reconstructed using the constrained model for a proof of concept.

6.1 Further work

Further testing of the algorithms detailed in this report needs to be done. Using a system of dedicated magnetometers with known magnetometer origin should be a first step. It would be interesting to first test the models in a undisturbed magnetic environment with accurate sensors and than gradually increase the magnetic disturbances to see how much of an impact the disturbances make. This would test how crucial it is that the assumption of the same bias field for all magnetometers is. It is probably primarily this assumption that limits the capability of the system in an ambulatory setting.

Another interesting thing would be to try to fuse the orientation and position estimate given by the system with the estimates given by the usual IMU approach. At first glance it could seem that the fact that the bias field is needed for the IMU estimation and that field is superpositioned on the dipole field from the permanent magnet rendering the usual IMU approach problematic. The static field is provided by the permanent magnet filter however and can be used in the IMU filter as a pseudo measurement.

Bibliography

M. Birsan. Non-linear kalman filters for tracking a magnetic dipole. *Technical Memorandum*, 2003. Cited on page 8.

J. Callmer, M. Skoglund, and F. Gustafsson. Silent localization of underwater sensors using magnetometers. *Eurasip Journal on Advances in Signal Processing*, 2010(709318), 2010. Cited on page 8.

F. Gustafsson. *Statistical sensor fusion*. Studentlitteratur, Lund, 2010. Cited on pages 10, 11, and 13.

F. Gustafsson and A.J. Isaksson. Best choice of coordinate system for tracking coordinated turns. In *Decision and Control, 1996., Proceedings of the 35th IEEE Conference on*, volume 3, pages 3145–3150 vol.3, 1996. doi: 10.1109/CDC.1996.573612. Cited on page 19.

A. Gut. *An intermediate course in probability*. Springer texts in statistics. Springer-Verlag New York, 2009. ISBN 9781441901620. Cited on page 11.

J.D. Hol. *Sensor Fusion and Calibration using Inertial Sensors, Vision, Ultra-Wideband and GPS*. Linköping Studies in Science and Technology. Dissertations No. 1368, Linköping University, Sweden, 2011. Cited on pages 25 and 26.

T. Kailath, A.H. Sayed, and B. Hassibi. *Linear estimation*. Prentice-Hall information and system sciences series. Prentice Hall, 2000. ISBN 9780130224644. Cited on pages 11 and 13.

M. Kok, J.D. Hol, T. Schön, F. Gustafsson, and H. Luinge. Calibration of a magnetometer in combination with inertial sensors. In *Proceedings of the 15th International Conference on Information Fusion (FUSION)*, pages 787–793. IEEE conference proceedings, 2012. Cited on pages 25 and 26.

J.B. Kuipers. *Quaternions and Rotation Sequences: A Primer With Applications to Orbits, Aerospace, and Virtual Reality*. Princeton paperbacks. Princeton Univers. Press, 2002. ISBN 9780691102986. Cited on pages 13 and 14.

D. Roetenberg. *Inertial and Magnetic Sensing of Human Motion*. PhD thesis, Enschede, may 2006. Cited on page 5.

D. Roetenberg, H.J. Luinge, C.T.M. Baten, and P.H. Veltink. Compensation of magnetic disturbances improves inertial and magnetic sensing of human body segment orientation. *IEEE Transactions on Neural Systems and Rehabilitation Engineering*, 13:395–405, 2005. Cited on page 7.

D. Roetenberg, P. Slycke, A. Ventevogel, and P.H. Veltink. A portable magnetic position and orientation tracker. *Sensors and Actuators A: Physical*, 135(2): 426–432, 2007a. URL `http://doc.utwente.nl/61421/`. Cited on page 7.

D. Roetenberg, P.J. Slycke, and P.H. Veltink. Ambulatory position and orientation tracking fusing magnetic and inertial sensing. *IEEE Transactions on Biomedical Engineering*, 54(5):883–890, 2007b. URL `http://doc.utwente.nl/61458/`. Cited on page 7.

H.M. Schepers. *Ambulatory assessment of human body kinematics and kinetics*. PhD thesis, Enschede, June 2009. Cited on page 5.

H.M. Schepers and P.H. Veltink. Stochastic magnetic measurement model for relative position and orientation estimation. *Measurement Science and Technology*, 21(6):065801, April 2010. Cited on page 7.

H.M. Schepers, D. Roetenberg, and P.H. Veltink. Ambulatory human motion tracking by fusion of inertial and magnetic sensing with adaptive actuation. *Medical and Biological Engineering and Computing*, 48(1):27–37, January 2010. Open Access. Cited on page 7.

T. Schon, F. Gustafsson, and A. Hansson. A note on state estimation as a convex optimization problem. In *Acoustics, Speech, and Signal Processing, 2003. Proceedings. (ICASSP '03). 2003 IEEE International Conference on*, volume 6, pages VI–61–4 vol.6, 2003. doi: 10.1109/ICASSP.2003.1201618. Cited on page 36.

D. Törnqvist. *Estimation and Detection with Applications to Navigation*. Linköping Studies in Science and Technology. Dissertations No. 1216, Linköping University, Sweden, 2008. Cited on pages 10 and 14.

N. Wahlström. Localization using magnetometers and light sensors, 2013. Cited on pages 8, 15, 16, and 17.

X. Yun and E.R. Bachmann. Design, implementation, and experimental results of a quaternion-based kalman filter for human body motion tracking. *Trans. Rob.*, 22(6):1216–1227, December 2006. ISSN 1552-3098. doi: 10.1109/TRO.2006.886270. URL `http://dx.doi.org/10.1109/TRO.2006.886270`. Cited on page 7.

H. Zhou and H. Hu. Human motion tracking for rehabilitation - a survey. *Biomedical Signal Processing and Control*, 3(1):1–18, 2008. Cited on page 7.

Linköpings universitet

Upphovsrätt

Detta dokument hålls tillgängligt på Internet — eller dess framtida ersättare — under 25 år från publiceringsdatum under förutsättning att inga extraordinära omständigheter uppstår.

Tillgång till dokumentet innebär tillstånd för var och en att läsa, ladda ner, skriva ut enstaka kopior för enskilt bruk och att använda det oförändrat för ickekommersiell forskning och för undervisning. Överföring av upphovsrätten vid en senare tidpunkt kan inte upphäva detta tillstånd. All annan användning av dokumentet kräver upphovsmannens medgivande. För att garantera äktheten, säkerheten och tillgängligheten finns det lösningar av teknisk och administrativ art.

Upphovsmannens ideella rätt innefattar rätt att bli nämnd som upphovsman i den omfattning som god sed kräver vid användning av dokumentet på ovan beskrivna sätt samt skydd mot att dokumentet ändras eller presenteras i sådan form eller i sådant sammanhang som är kränkande för upphovsmannens litterära eller konstnärliga anseende eller egenart.

För ytterligare information om Linköping University Electronic Press se förlagets hemsida `http://www.ep.liu.se/`

Copyright

The publishers will keep this document online on the Internet — or its possible replacement — for a period of 25 years from the date of publication barring exceptional circumstances.

The online availability of the document implies a permanent permission for anyone to read, to download, to print out single copies for his/her own use and to use it unchanged for any non-commercial research and educational purpose. Subsequent transfers of copyright cannot revoke this permission. All other uses of the document are conditional on the consent of the copyright owner. The publisher has taken technical and administrative measures to assure authenticity, security and accessibility.

According to intellectual property law the author has the right to be mentioned when his/her work is accessed as described above and to be protected against infringement.

For additional information about the Linköping University Electronic Press and its procedures for publication and for assurance of document integrity, please refer to its www home page: `http://www.ep.liu.se/`

© Jacob Antonsson